



Influence of fibre type and dipping cycle on graphene adsorption and electrical conductivity of fibres

Vinit Kumar Jain & Arobindo Chatterjee^a

Department of Textile Technology, Dr BR Ambedkar National Institute of Technology Jalandhar, Jalandhar 144 011, India

Received 15 July 2020; revised received and accepted 20 November 2020

The influence of fibre type and dipping cycle on the graphene oxide (GO) add-on and the resultant mass-specific resistance has been studied for different fibres. Seven commonly used fibres, viz cotton, viscose, silk, wool, nylon, acrylic and polyester, are selected for the study. A comparative evaluation of GO add-on and the resultant mass-specific resistance of all these fibres are carried out under similar process conditions. Fibres are treated separately with 1% w/v GO solution up to 10 consecutive dipping cycles. Graphene oxide enriched fibres are reduced with sodium dithionite to restore graphene structure. Use of fibre as substrate for experiment eliminates the effect of other structural parameters of either yarn or fabric form. FTIR and UV-vis spectra confirm successful exfoliation of graphite to GO. FTIR study reveals significant chemical interaction of GO with cotton, viscose, nylon, and silk. SEM micrographs show that the graphene sheets are uniformly deposited on the cotton, silk, and nylon. Cotton yields maximum GO add-on and acrylic yields the lowest in all dipping cycles. Lowest mass-specific resistance is obtained in case of cotton, while highest values are obtained in case of acrylic after 10 dipping cycles. Nylon needs lowest amount to GO to achieve the same level of conductivity.

Keywords: Acrylic, Cotton, Electrical conductivity, Graphene oxide, Mass-specific resistance, Nylon, Polyester, Silk, Viscose, Wool

1 Introduction

Electrically conductive textile (E-textile) have attracted great interest in recent year due to its vast applications in wearable electronic devices, health and activity monitoring devices, energy reservoir, etc¹. Conventionally metal coating, metal particles or metal threads are incorporated during fibre formation, yarn formation, weaving or embroidery to impart electrical conductivity in otherwise insulating textile media. Trending approach is the application of conjugated polymers and carbon based conductive material (carbon nanotubes, carbon black and graphene) via surface coating and polymer blending during spinning. Unlike metals, these electro-conductive textiles will be flexible, durable, moldable, and light-weight¹⁻⁵. The most spectacular quality of these novel electro-conductive textiles will be the ability to tailor-made conductivity as per the requirement to suit a specific application. Successful application of these polymers onto textile materials will yield electro-conductive textiles which will possess synergistic properties of both the conductive polymer and textiles and may open up many potential

applications. Graphene is discovered by Physicists Andre Geim and Konstantin Novoselov of the University of Manchester in 2004 which earned them Nobel Prize in Physics in 2010⁶. It has a flat monolayer of carbon atoms bound together with double electron bonds (termed as sp² bond) which is tightly packed into a two-dimensional honeycomb lattice. Due to its outstanding electronic, optical, thermal and mechanical properties, it has attracted great interest as an outstanding candidate for the production of advanced materials with much potential in various applications^{7,8}. It has been demonstrated that aqueous dispersions of GO can readily be produced without the need of any stabilizers due to the presence of carboxylic and hydroxyl groups in it⁹. This advantage leads to the possible direct application of graphene in preparing electro-conductive textiles using simple dip-nip process. Application of graphene onto textile substrates will yield a functional composite which will have synergistic properties of both graphene and textiles¹⁰.

Graphene has advantages over other conductive materials, such as carbon nanotubes and conductive polymers, in terms of the fabrication of electro-conductive textiles^{11,12}. Graphene based electro-conductive textiles can be explored for various

^aCorresponding author.
E-mail: chatterjeea@nitj.ac.in

potential applications such as flexible sensors or wearable electronics, EMI shielding, etc. It can also be used for the development of anti-microbial fabric, hydrophobic fabric, chemical and UV resistance fabric, reinforcement of polymers, saline or effluent water treatment, etc.¹³. Though pristine graphene, exfoliated by mechanical method, is more electrically conductive than chemically reduced graphene, but it cannot be applied on textile substrate due to its lack of chemical functionalities and affinity¹⁴. Affinity of graphene towards textile substrate is required for adequate and durable fixation. Therefore, it is important to understand the interaction or affinity of graphene with textile materials to identify suitable substrate for development of graphene based electro conductive textile. Strong oxidizing agents expand graphite layers and incorporates oxygenated functionalities which makes the material hydrophilic in nature, thereby increasing its affinity towards textile material. Nature of functional group (active sites) of fibre which determines their surface charge in aqueous medium has strong impact on graphene loading on fibre surface¹⁵. Graphene oxide carries a strong negative charge in aqueous solution due to deprotonation of carboxyl (-COOH) and hydroxyl (-OH) groups on GO basal plane¹⁶. Textile fibres acquire negative surface charge in neutral aqueous media. Despite the electrostatic repulsion between anionic surface functionalities of fibre and GO, graphene add-on on fibre surface is explained based on non-electrostatic forces, such as hydrophobic, π - π type interactions, Lifshitz van der Waals, and hydrogen bonding¹⁷. In literature, most of the studies related to graphene coated textile are confined in either yarn or fabric form, such as woven, nonwoven and knitted structures¹⁸⁻²⁰. With these form of substrates, it is difficult to understand the inherent affinity of graphene towards the fibre material itself as there are several other structural parameters, such as pore size, degree of openness of yarn, fabric surface, etc., which may influence graphene add-on. Comparative graphene affinity of different textile materials can be judged more precisely when textile substrates are used in loose fibre form and without any surface modification. Therefore, the aim of the present study is to investigate the influence of fibre type and dipping cycle on graphene add-on and the resultant mass-specific resistance.

2 Materials and Methods

2.1 Materials and Reagents

Graphite powder (particle size ~ 44 microns) is procured from Alfa Aesar (U.K.). Analytical grade sulfuric acid (H_2SO_4), phosphoric acid (H_3PO_4), sodium hydrosulfite ($Na_2S_2O_4$), potassium permanganate ($KMnO_4$), hydrogen peroxide (H_2O_2), hydrochloric acid (HCl), and ethanol are procured from S D Fine Chem Limited (India). Milli-Q grade (resistivity of $13 M\Omega.cm.$) deionized water is used throughout the experiments. Cotton, viscose, silk, wool, nylon, acrylic and polyester in fibre form are used as substrate. The technical parameters of the fibres used are shown in Table 1.

2.2 Preparation of GO Coated Textile Fibres

Graphene oxide, synthesised by improved hummers' method²¹ is rinsed with 5 % HCl, ethanol and deionized water until the attainment of pH 4.2. Stock solution of aqueous GO dispersion of 1 % concentration is prepared with deionized water. For preparation of GO coated fibres, measured quantity of stock solution, as per M:L ratio, is sonicated for 30 min at 30 °C, amplitude 60% and pulse 10:10²². Scoured fibres²³ are soaked in the sonicated GO dispersion (M:L ratio 1:50) for 30 min at 70 °C and then dried at 75 °C for each dipping cycle. The procedure is repeated for consecutive 5 cycles and 10 cycles to obtain GO coated fibres at different dipping cycles. Three different dipping cycles (1, 5 and 10) are used for the study. Finally, GO treated fibre are reduced with sodium dithionite solution of concentration 50 mM at 95 °C for 30 min, M:L ratio of 1:100 and subsequently dried at 100 °C¹⁰.

2.3 Measurement Methods

UV-visible spectra of GO and reduced graphene oxide (RGO) are recorded in the range of 220-800 nm (UV-2600, Shimadzu UV-VIS Spectrometer). ATR-FTIR analysis of graphite, GO, RGO and GO coated

Table 1 — Technical parameter of fibres

Fibres	Linear density	Surface area, m ² /g
Cotton	4.2 micronaire	0.2237
Viscose	1.3 decitex	0.2547
Silk	1.0 denier	0.2920
Nylon	1.5 denier	0.2571
Acrylic	2.0 denier	0.2180
Polyester	1.4 denier	0.2411
Wool	20 micron	0.1501

fibre samples are conducted in a spectrometer (Carry 630, Agilent Technologies) within the wave number range of 400-4000 cm^{-1} . Surface micrographs of GO coated textiles are recorded with JEOL SEM analyzer model no- JSM -6510 LV. Magnifications ranging from $\times 1000$ to $\times 10,000$. Graphene add-on per unit surface area of fibre is measured to compare GO loading of different fibre substrates. Add-on per unit surface area is defined as the increase in weight of the fibre after treatment on the initial weight of the fibre with respective to per unit surface area, as shown below:

$$\text{Add-on per unit surface area (mg m}^{-2}\text{)} = \frac{W_{gf} - W_f}{\pi dl}$$

where W_{gf} is the oven dry weight of GO coated fibre sample; W_f , the oven dry weight of fibre sample; d , the diameter of fibre in metre; and l , the length of fibre in metres.

To eliminate the effect of variability in fibre cross-section, electrical resistance is calculate as mass-specific resistance. Mass-specific resistance is calculated using the following formula:

$$R_s = \rho \times d \quad \dots (1)$$

where ρ is the electrical resistivity; and d , the density of material in g/cm^3 , as shown below:

$$\rho = \frac{R \times A}{l} \quad \dots (2)$$

where A is the cross-section area; and l , the length of fibre, as given below:

$$A = \frac{\text{tex}}{d \times 10^5} \quad \dots (3)$$

Mass-specific resistance of fibre can be express as

$$R_s = \frac{R \times N \times \text{tex}}{l \times 10^5} \quad \dots (4)$$

where l is the distance between the ends of the specimen (cm); N denotes number of fibres; and R_s , the mass-specific resistance in $\Omega \text{ g cm}^{-224,25}$.

Electrical resistance (R) is measured with two probe digital multimeter (MASTEC[®] MAS830L) for 1 cm length of fibre. Each experiment is replicated 5 times and their mean is plotted with standard deviation (SD). The Student's T-test (T-test) is

employed to analyse the statistical significance test at confidence level of 95% ($p < 0.05$).

3 Results and Discussion

3.1 UV-visible Spectra of GO and RGO

UV-vis absorption spectra of GO and RGO are shown in Fig.1. Maximum wavelength absorption in GO, recorded at 229 nm is attributed to $\pi \rightarrow \pi^*$ transitions of aromatic C-C bonds, which indicates functionalization of graphite with oxygenated functionalities²⁶. After the reduction with sodium dithionite the 229 nm peak is red shifted to 264 nm which indicates partial restoration of graphene π - π conjugation network²⁷⁻²⁹.

3.2 Fourier Transform Infra-red Spectroscopy Analysis

FTIR spectra of graphite powder, GO and RGO are shown in Fig.2(a). Vibrational mode spectrum of GO illustrates two characteristic peaks at 1635 cm^{-1} and 3308 cm^{-1} , corresponding to stretching vibrations of C=O and O-H respectively, indicating exfoliation of graphite powder to amphiphilic GO^{30,31}. The absence of all these vital peaks in the RGO spectrum implies chemical reduction of GO to graphene. New small band at 1513 cm^{-1} in RGO spectrum is attributed to skeletal vibration of graphene nanosheets³².

Significant changes are observed in FTIR spectra of GO coated cotton (GO-cotton), GO coated viscose (GO-viscose), GO coated silk (GO-silk) and GO coated nylon (GO-nylon) compared to respective untreated fibres. The FTIR spectra of cotton and GO-cotton are shown in Fig. 2(b). In GO-cotton spectra two new bands appear at 1643 cm^{-1} and 1546 cm^{-1} , corresponding to C=C unoxidized sp^2 bond and skeletal vibration of graphene nanosheets^{5,33}.

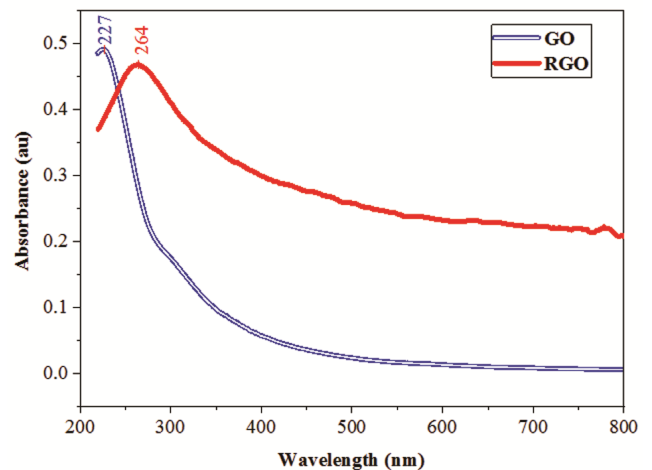


Fig. 1 — UV- vis absorption spectra of GO and RGO

Moreover, the C-H stretch at 2896 cm^{-1} is red shifted to 2872 cm^{-1} suggesting intermolecular hydrogen bond formation between cotton and GO. The FTIR spectra of viscose and GO-viscose is shown in Fig. 2(c). The appearance of a weak band at 1565 cm^{-1} in the GO-viscose spectra may be assigned to C=C skeletal vibration of graphene nanosheets. Absorption of GO broadens and red shifts the OH

stretch from 3303 cm^{-1} to 3250 cm^{-1} . This observation indicates interaction between carbonyl group and hydroxyl group of GO and hydroxyl group of viscose through hydrogen bonds.

Figure 2(d) shows the FTIR spectra of silk and GO-silk. Three typical adsorption band of amide-I ($1700\text{-}1600\text{ cm}^{-1}$), amide-II ($1560\text{-}1500\text{ cm}^{-1}$) and amide-III ($1300\text{-}1200\text{ cm}^{-1}$) can be seen in the spectra

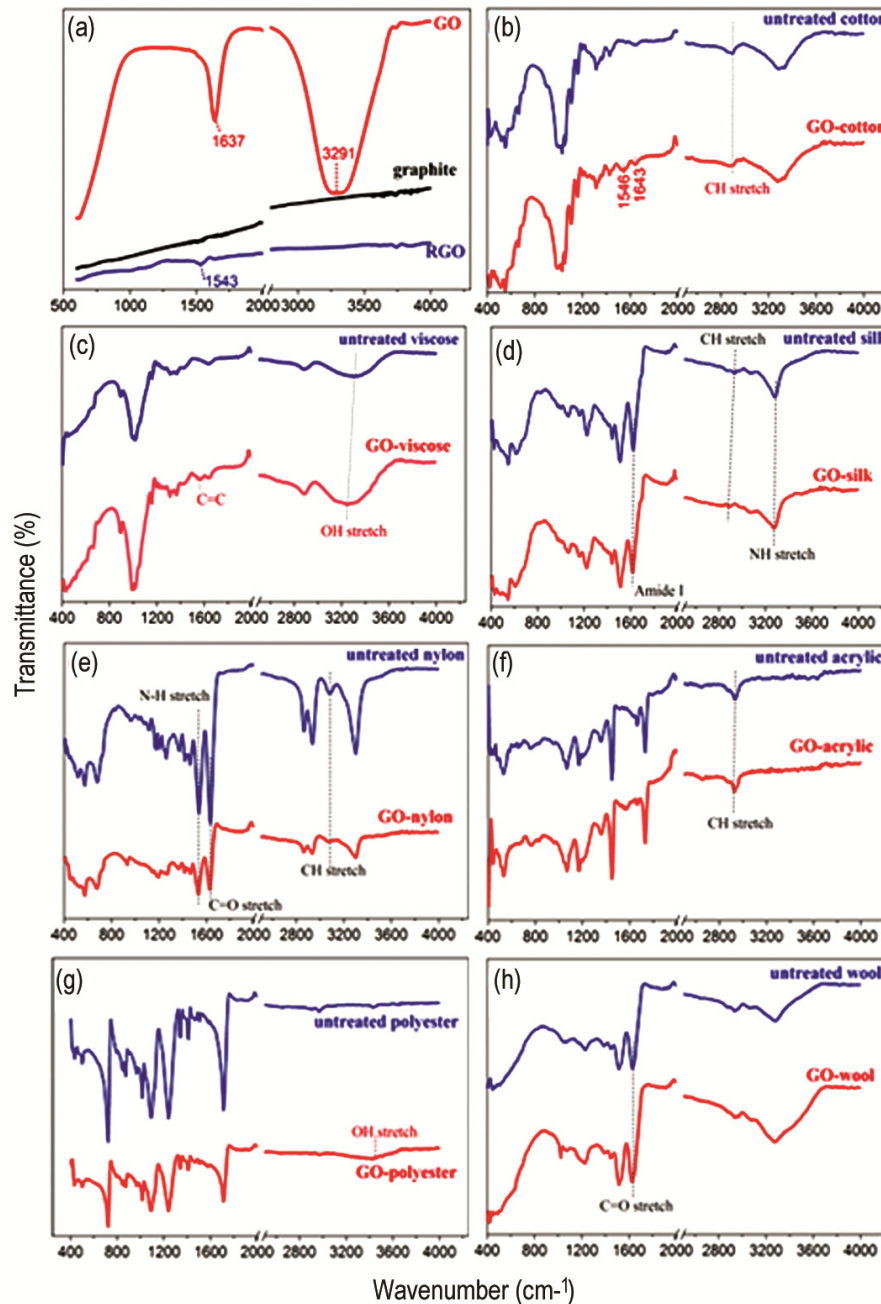


Fig. 2 — FTIR spectra of (a) graphite powder, GO and RGO, (b) untreated cotton and GO-cotton, (c) untreated viscose and GO-viscose, (d) untreated silk and GO-silk, (e) untreated nylon and GO-nylon, (f) untreated acrylic and GO-acrylic, (g) untreated polyester and GO-polyester and (h) untreated wool and GO-wool

of untreated silk. After GO deposition, the C-H stretching peak at 2934 cm^{-1} and amide-I band at 1622 cm^{-1} are red shifted to 2886 cm^{-1} and 1618 cm^{-1} (ref³⁰). The red shifting of N-H stretch vibration from 3281 cm^{-1} to 3273 cm^{-1} indicates chemical interaction of GO with silk via hydrogen bonding³⁴. Figure 2(e) shows the FTIR spectra of nylon and GO-nylon. It is clearly seen that the peaks arising due to C-H asymmetric stretching vibration in untreated nylon are red shifted from 3080 cm^{-1} to 3066 cm^{-1} after GO deposition. Further, the C=O stretch and N-H bend are also red shifted from 1634 cm^{-1} to 1629 cm^{-1} and from 1538 cm^{-1} to 1533 cm^{-1} . This red shifting of vital peaks indicates intermolecular hydrogen bonding between nylon and GO³⁵.

In case of acrylic, the peak arising due to C-H stretch is red shifted from 2931 cm^{-1} to 2926 cm^{-1} after GO deposition [Fig. 2(f)]. The spectrum of GO-polyester shows a new broad absorption band at 3428 cm^{-1} due to GO deposition [Fig. 2(g)]. FTIR spectra of wool show red shifting of C=O stretch from 1629 cm^{-1} to 1625 cm^{-1} after GO deposition [Fig. 2(h)].

Based on the above observations, it can be inferred that there is no significant interaction of GO with acrylic, polyester and wool for the particular conditions of sample preparation used during the study. A schematic representation of the possible modes of interaction among GO with cotton/viscose, silk and nylon are shown in Fig. 3.

3.3 SEM Analysis of GO Coated Textile Fibre

The SEM images of the GO coated fibres are illustrated in Fig. 4. Important observations from the SEM analysis are summarised hereunder.

Higher GO add-on is observed in cotton as compared to those in other fibres. Relatively uniform distribution of GO sheets is found on cotton, silk and nylon. Localised distribution of GO is found in case of viscose. GO add-on in case of viscose is non-uniform and it seems that the add-on is primarily due the attachment of GO with the previously present GO on the surface of the fibre. It can be observed that the adsorption of GO sheets on wool, polyester and acrylic are relatively poor and non-uniform. Surface damage can also be noticed in GO-cotton and GO-viscose, which may be due to acid hydrolysis [Figs 5(a) & (b)].

3.4 Comparative Assessment of Graphene Add-on on Fibres

Dipping cycle vs. add-on curves for different fibres are shown in Fig. 6(a). For first dipping cycle, maximum graphene add-on per unit surface area is observed in case of cotton (15.65 mg m^{-2}) followed by silk (13.00 mg m^{-2}), viscose (4.32 mg m^{-2}), nylon (3.75 mg m^{-2}), wool (3.24 mg m^{-2}), acrylic (2.19 mg m^{-2}) and polyester (2 mg m^{-2}). It can be clearly seen that the initial graphene add-on per unit surface area is much higher in case of cotton and silk as compared to other fibres.

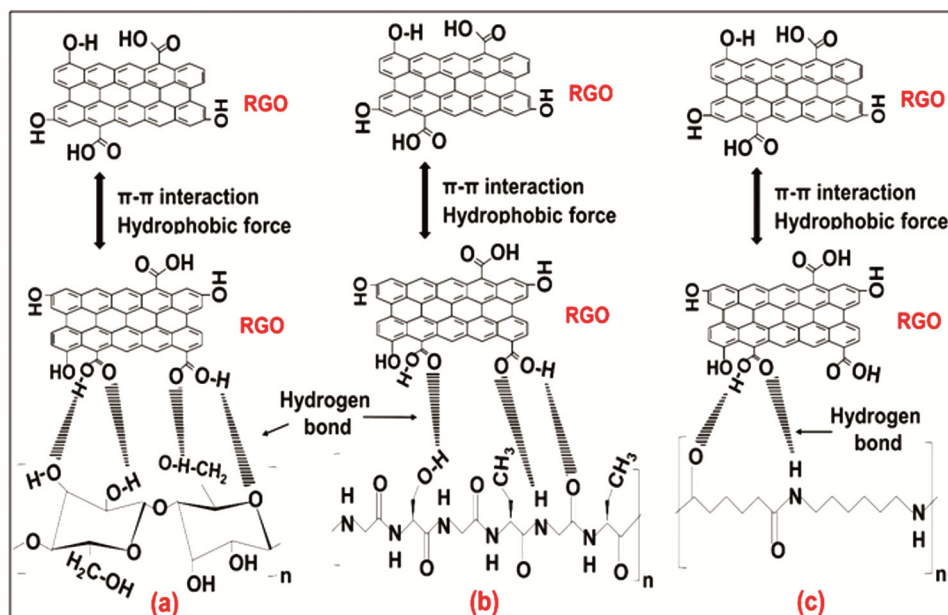


Fig. 3 — Schematic representation of possible modes of interaction between GO with (a) cotton/viscose, (b) silk, and (c) nylon

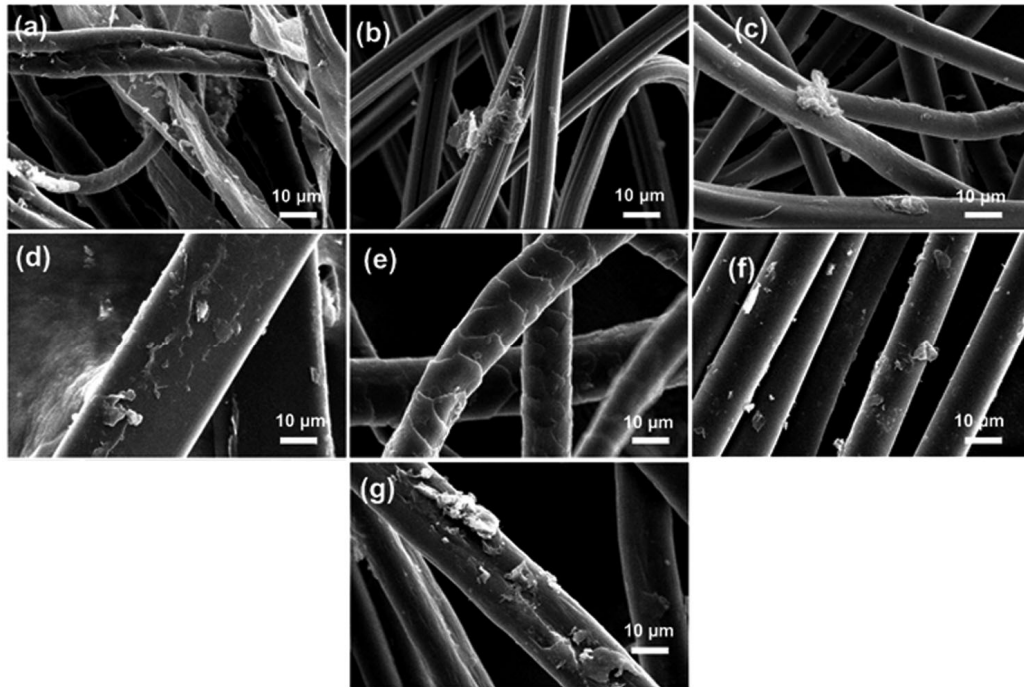


Fig. 4 — SEM image of (a) GO-cotton, (b) GO-viscose, (c) GO-silk, (d) GO-nylon, (e) GO-wool, (f) GO-polyester and (g) GO-acrylic

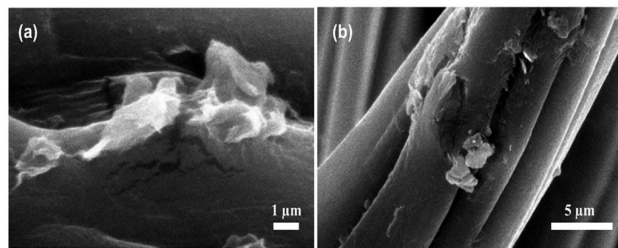


Fig. 5—Surface damage of (a) GO-cotton and (b) GO-viscose

On further increasing the dipping cycle to 5, there is a sharp increase in graphene add-on in case of cotton (113.55 mg m^{-2}) and silk (60.92 mg m^{-2}) followed by viscose (28.34 mg m^{-2}), nylon (28 mg m^{-2}), wool (19.79 mg m^{-2}), polyester (9.96 mg m^{-2}) and acrylic (4.20 mg m^{-2}). Going from 5 dipping cycles to 10 dipping cycles, there is a reduction in rate of increase in graphene add-on in case of cotton and silk, whereas viscose exhibit a steep rise in graphene add-on and it overtakes silk in terms of graphene yield per unit surface area. Irrespective of the number of dipping cycles, cotton always exhibits maximum graphene yield per unit surface area. Viscose, silk and nylon are next to cotton in terms of graphene add-on after 10 dipping cycles. The values of the graphene add-on for different fibres after 10 dipping cycles are cotton

(151.10 mg m^{-2}) followed by viscose (108.09 mg m^{-2}), silk (95.55 mg m^{-2}), nylon (67.44 mg m^{-2}), wool (31.57 mg m^{-2}), polyester (19.85 mg m^{-2}) and acrylic (7.88 mg m^{-2}).

Graphene oxide mass loading on textile substrates in fibre form are not reported earlier. Previously reported literature are related to GO mass loading on textile substrate in fabric or yarn form as well as with surface modification. Moreover, GO add-on on textile substrate in fabric form are reported in literature for cotton, nylon and polyester. Therefore, these forms of data are not comparable with the findings of the present study as the form of substrate as well as surface modifications influence the GO add-on. However, our experimental results reasonably match with the reported value for cotton (3.31% and 1.08 mg cm^{-2})^{18,36}, nylon (2.3 mg cm^{-2})³⁷ and polyester (0.38 mg g^{-1})³⁸.

Initial graphene adsorption on fibre is due to the interaction of GO and functional groups of fibre where available and/or through electrostatic, hydrophobic, van der Waals, and pie interaction. Further adsorption is primarily due to the π - π interaction and hydrophobic force between the GO in solution and GO already present on the surface of the fibre and/or may also be due to interaction of GO with remaining free functional groups of fibre.

For the fibres used in the study, cotton and viscose have similar chemical structure; silk, wool and nylon have some common functional groups, and polyester and acrylic do not have any functional groups. Between cotton and viscose, cotton always exhibits considerably higher graphene add-on than that of viscose although they are of same chemical nature and moreover viscose is more amorphous compared to cotton. Higher graphene add-on in case of cotton may be due to presence of convolution, which may act as anchoring point for the deposition of graphene. Based on the above observations, it may be assumed that surface texture or nature of surface may play an important role in influencing the graphene add-on.

Among silk, nylon and wool, wool exhibits considerably low graphene add-on which may be due to the presence of hydrophobic scales on fibre surface. It can also be seen from the SEM image [Fig. 4(e)] that in case of wool the deposition of the graphene is mainly around the edge of the scale, which further strengthen the assumption that the surface texture of fibre may have a role to play in the process of graphene add-on.

3.5 Comparative Assessment of Mass-specific Resistance for GO Coated Fibres

Prior to GO treatment, the mass-specific resistance of the fibres are very high and outside the measuring range of the instrument used to measure the same. However, the reported values²⁵ of the mass-specific resistance of these fibres at 65% relative humidity are as follows: cotton $10^{6.8} \Omega \text{ g cm}^{-2}$, viscose $10^7 \Omega \text{ g cm}^{-2}$, silk $10^{9.8} \Omega \text{ g cm}^{-2}$, nylon $10^{9-12} \Omega \text{ g cm}^{-2}$, wool $10^{8.4-9.9} \Omega \text{ g cm}^{-2}$, acrylic $10^{8.7} \Omega \text{ g cm}^{-2}$ and polyester $10^8 \Omega \text{ g cm}^{-2}$.

With graphene add-on, the mass-specific resistance of all the fibres decreases but in case of wool, acrylic and polyester the graphene add-on is low as well as the resultant values of the mass-specific resistance are relatively high. Therefore, the change in mass-specific resistance with dipping cycle is shown in Fig. 6(b) for cotton, viscose, silk and nylon.

After 10 dipping cycles, lowest mass-specific resistance is achieved in cotton ($112.15 \Omega \text{ g cm}^{-2}$) followed by viscose ($124.87 \Omega \text{ g cm}^{-2}$), silk ($147.46 \Omega \text{ g cm}^{-2}$), nylon ($160.53 \Omega \text{ g cm}^{-2}$), wool ($694 \Omega \text{ g cm}^{-2}$), polyester ($747.65 \Omega \text{ g cm}^{-2}$) and acrylic ($887.24 \Omega \text{ g cm}^{-2}$).

Literature related to electrical resistivity measurement of GO coated textile substrates are confined in surface resistivity and linear resistivity

because of the fabric or yarn form of substrate. However, mass-specific resistance of polypyrrole (PPy) coated cotton yarn, wool yarn and nylon yarn are reported as $1.53 \Omega \text{ g cm}^{-2}$, $1.69 \Omega \text{ g cm}^{-2}$ and $2.59 \Omega \text{ g cm}^{-2}$ respectively. The mass-specific resistance of PPy coated cotton, wool and nylon yarns are relatively lower than the obtained GO coated cotton, wool and nylon fibres, may be due to the yarn form of substrate²⁴.

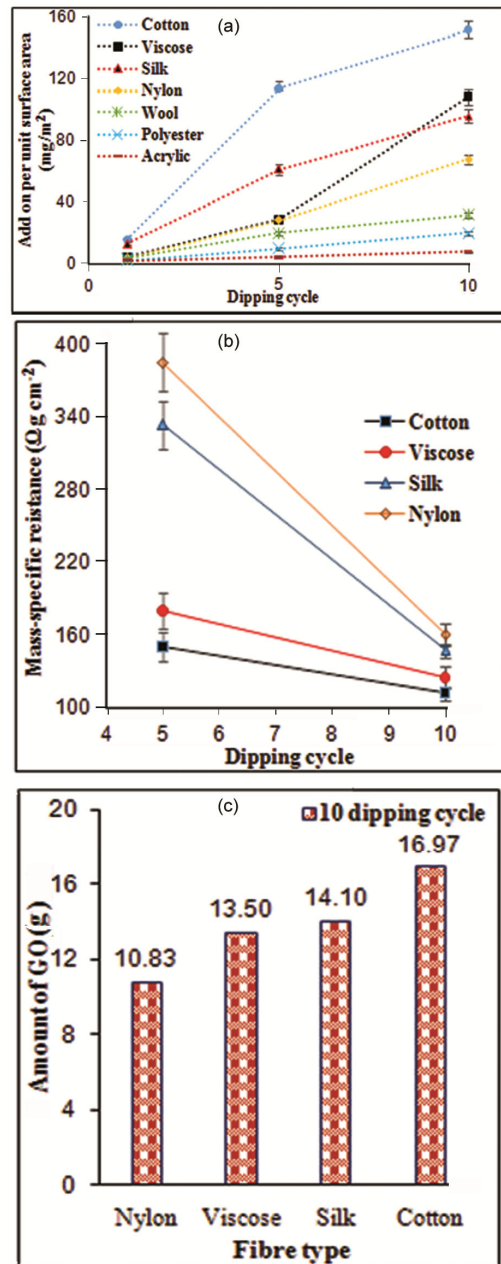


Fig. 6— (a) Influence of dipping cycle on graphene add-on, (b) influence of dipping cycle on mass-specific resistance and (c) amount of GO required to achieve $1 \Omega \text{ g cm}^{-2}$ mass specific resistance

Increasing dipping cycle results in improvement of GO loading and reduction of the mass-specific resistance of fibres. Lowest mass-specific resistance is achieved in cotton ($112.15 \Omega \text{ g cm}^{-2}$) at 10 dipping cycle. Mass-specific resistance of viscose decreases from $180.49 \Omega \text{ g cm}^{-2}$ to $124.87 \Omega \text{ g cm}^{-2}$ with increasing dipping cycle from 5 cycles to 10 cycles. Significant difference in mass-specific resistance of cotton and viscose at 10 dipping cycle is observed (p value = 0.035). It is worth mentioning that in case of nylon, a reasonably low mass-specific resistance of $160.53 \Omega \text{ g cm}^{-2}$ can be achieved at a relatively low graphene add-on of 67.44 mg m^{-2} . A low mass-specific resistance against a low graphene add-on suggests that nylon may be an economical substrate for electro-conductive biomedical application where application of cotton is restricted.

3.6 Relationship between Graphene Add-on and Mass-specific Resistance

In case of cotton, increasing dipping cycle from 5 to 10 leads to a 33 % increase in graphene add-on per unit surface area and 25.7 % reduction in mass-specific resistance. In case of viscose increasing dipping cycle from 5 to 10 shows 281.4 % increase in graphene add-on per unit surface area and 30.82 % reduction in mass-specific resistance is observed. Though in case of viscose there is 281.4% increase in graphene add-on after 10 cycle but the corresponding reduction in mass-specific resistance is not that large or is not proportionate to the increase in graphene add-on. This may be due to a relatively non-uniform deposition of graphene on viscose. From SEM image [Fig. (4b)], it can be clearly observed that graphene add-on in case of viscose is non-uniform and increase in the graphene add-on is primarily due the attachment of graphene with the previously present graphene on the surface of the fibre. Increasing dipping cycle from 5 to 10 shows about 140.86 % increase in graphene add-on per unit surface area in case of nylon. Subsequently, mass-specific resistance is decreased to 58.33 %.

In case of silk, with the increase in dipping cycle from 5 to 10, the graphene add-on per unit surface area increases to 56.85 % and mass-specific resistance is decreased to 55.81 %. In case of polyester and acrylic, the graphene add-on is not appreciable even after 10 dipping cycles. This is because hydrophobic fibre surface have lower specific amount of charge due to less amount of functional group on surface (thin electric double layer) as

compared to hydrophilic fibre³⁹. In order to have a comprehensive understanding about graphene add-on and the resultant mass-specific resistance of different fibres, a relative comparison is made on the basis of GO requirement to achieve same level of conductivity. To calculate the amount of GO required to achieve $1 \Omega \text{ g cm}^{-2}$ mass-specific resistance, the graphene add-on per unit surface area is multiplied with mass-specific resistance. It is assumed that mass-specific resistance linearly decreases with the increase in graphene add-on. Figure 6(c) represents the predicted values of GO add-on (g) on the basis of 10 dipping cycle experimental data. On the basis of GO required to achieve same level of conductivity, nylon is identified as the best substrate. Compared to other fibres, nylon needs lowest amount of GO (10.83 g) to achieve $1 \Omega \text{ g cm}^{-2}$ mass-specific resistance at 1 m^2 fibre surface area.

4 Conclusion

Graphene oxide coated cotton, viscose, silk, nylon, wool, polyester and acrylic are successfully prepared by dipping the substrate in GO aqueous dispersion. UV-vis spectra and FTIR spectra of GO reveals successful chemical exfoliation of graphite. Mass-specific resistance decreases with increasing the number of dipping cycle. Cotton yields highest add-on per unit surface area and lowest mass-specific resistance in all dipping cycles. Silk yields second highest graphene add-on up to 5 cycles and on further increasing dipping cycle viscose replaces silk. From the response of the cotton and wool, it may be assumed that fibre surface texture has a role to play in the process of graphene adsorption. On the basis of GO required to achieve same level of conductivity, nylon is identified as the best substrate. SEM micrographs show that GO sheets are relatively uniformly deposited on the cotton, silk and nylon. Surface damage is observed in cotton and viscose. Poor interaction of GO with wool, polyester and acrylic is also observed.

References

- 1 Lund A, van der Velden N M, Persson N K, Hamed M M & Müller C, *Mater Sci Eng R: Reports*, 126 (2018) 1.
- 2 Malhotra U, Maity S & Chatterjee A, *J Appl Polym Sci*, 132 (2015) 1.
- 3 Maity S, Chatterjee A, Singh B & Pal Singh A, *J Text Inst*, 105 (2014) 887.
- 4 Chatterjee A, Maity S, Rana S & Figueiro R, in *Fibrous and Textile Materials for Composite Applications*, edited by S Rana & R Figueiro (Springer Science+Business Media, Singapore), 2016, 317.

- 5 Chatterjee A & Maity S, in *Advanced Textile Engineering Materials*, edited by Shahid-ul-Islam & B S Butola (Scrivener Publishing LLC, USA), 2018, 177.
- 6 Geim AK & Novoselov KS, *Nat Mater*, 6 (2007) 183.
- 7 Allen MJ, Tung VC & Kaner RB, *Chem Rev*, 110 (2010) 132.
- 8 Kuila T, Bose S, Mishra AK, Khanra P, Kim NH & Lee JH, *Prog Mater Sci*, 57 (2012) 1061.
- 9 Konkena B & Vasudevan S, *J Phys Chem Lett*, 3 (2012) 867.
- 10 Shateri-Khalilabad M & Yazdandshenas ME, *Carbohydr Polym*, 96 (2013) 190.
- 11 Shateri-Khalilabad M & Yazdandshenas ME, *Cellulose*, 20 (2013) 963.
- 12 Molina J, Fernández J, del Río AI, Bonastre J & Cases F, *Appl Surf Sci*, 279 (2013) 46.
- 13 Javed K, Galib CMA, Yang F, Chen CM & Wang C, *Synth Met*, 193 (2014) 41.
- 14 Dreyer DR, Park S, Bielawski CW & Ruoff RS, *Chem Soc Rev*, 39 (2010) 228.
- 15 Grancarić AM, Ristić N, Tarbuk A & Ristić I, *Fibres Text East Eur*, 21 (2013) 106.
- 16 Sahito IA, Sun KC, Arbab AA, Qadir MB & Jeong SH, *Carbohydr Polym*, 130 (2015) 299.
- 17 Giménez-Martín E, López-Andrade MA & Campos D, *J Text Inst*, 5000 (2018) 1.
- 18 Chatterjee A, Nivas Kumar M & Maity S, *J Text Inst*, 108 (2017) 1910.
- 19 Tang X, Tian M, Qu L, Zhu S, Guo X, Han G, Sun K, Hu X, Wang Y & Xu X, *Synth Met*, 202 (2015) 82.
- 20 Molina J, *RSC Adv*, 6 (2016) 68261.
- 21 Marcano DC, Kosynkin D V, Berlin JM, Sinitskii A, Sun Z, Slesarev A, Alemany LB, Lu W & Tour JM, *ACS Nano*, 4 (2010) 4806.
- 22 Tissera ND, Wijesena RN, Perera JR, Silva KMN De & Amaratunge GAJ, *Appl Surf Sci*, 324 (2015) 455.
- 23 Karmakar S R, *Chemical Technology in the Pre-treatment Processes of Textiles* (Elsevier Science), 1999, 86.
- 24 Kaynak A, Shaikhzadeh S & Foitzik RC, *Synth Met*, 158 (2008) 1.
- 25 Morton WE & Hearle JWS, *Physical Properties of Textile Fibres* (The Textile Institute, Manchester) 2008, 643.
- 26 Çiplak Z, Yildiz N & Çalimli A, *Fullerenes, Nanotub Carbon Nanostructures*, 23 (2015) 361.
- 27 Gurunathan S, Woong Han J, Eppakayala V & Kim J, *Int J Nanomedicine*, 8 (2013) 1015.
- 28 Huang NM, Chang & Huang NM, *Int J Nanomedicine*, 7 (2012) 3379.
- 29 Johra FT, Lee JW & Jung WG, *J Ind Eng Chem*, 20 (2014) 2883.
- 30 Pavia DL, Lampman GM, Kriz GS & Vyvyan JR, *Introduction to Spectroscopy* (Cengage Learning India Pvt. Ltd., New Delhi), 2015, 29.
- 31 Sahito IA, Sun KC, Arbab AA, Qadir MB & Jeong SH, *Electrochim Acta*, 173 (2015) 164.
- 32 Ouadil B, Cherkaoui O, Safi M & Zahouily M, *Appl Surf Sci*, 414 (2017) 292.
- 33 Cao J & Wang C, *Appl Surf Sci*, 405 (2017) 380.
- 34 Chitichotpanya P & Chitichotpanya C, *Coatings*, 7 (2017) 145.
- 35 Jung MR, Horgen FD, Orski S V, Rodriguez C V, Beers KL, Balazs GH, Jones TT, Work TM, Brignac KC, Royer S, Hyrenbach KD, Jensen BA & Lynch JM, *Mar Pollut Bull*, 127 (2018) 704.
- 36 Liu W, Yan X, Lang J, Peng C & Xue Q, *J Mater Chem*, 22 (2012) 17245.
- 37 Zhao C, Shu K, Wang C, Gambhir S & Wallace GG, *Electrochim Acta*, 172 (2015) 12.
- 38 Moleon JA, Ontiveros-Ortega A, Gimenez-Martin E & Plaza I, *Dye Pigm*, 122 (2015) 310.
- 39 Grancarić AM, Tarbuk A & Pusic T, *Color Technol*, 121 (2005) 221.